

# Intracellular distribution of nontargeted quantum dots after natural uptake and microinjection

Leona Damalakiene<sup>1</sup>  
Vitalijus Karabanovas<sup>2</sup>  
Saulius Bagdonas<sup>1</sup>  
Mindaugas Valius<sup>3</sup>  
Ricardas Rotomskis<sup>1,2</sup>

<sup>1</sup>Biophotonics Group, Laser Research Center, Faculty of Physics, <sup>2</sup>Biomedical Physics Laboratory, Institute of Oncology, <sup>3</sup>Proteomics Center, Institute of Biochemistry, Vilnius University, Vilnius, Lithuania

**Background:** The purpose of this study was to elucidate the mechanism of natural uptake of nonfunctionalized quantum dots in comparison with microinjected quantum dots by focusing on their time-dependent accumulation and intracellular localization in different cell lines.

**Methods:** The accumulation dynamics of nontargeted CdSe/ZnS carboxyl-coated quantum dots (emission peak 625 nm) was analyzed in NIH3T3, MCF-7, and HepG2 cells by applying the methods of confocal and steady-state fluorescence spectroscopy. Intracellular colocalization of the quantum dots was investigated by staining with Lysotracker®.

**Results:** The uptake of quantum dots into cells was dramatically reduced at a low temperature (4°C), indicating that the process is energy-dependent. The uptake kinetics and imaging of intracellular localization of quantum dots revealed three accumulation stages of carboxyl-coated quantum dots at 37°C, ie, a plateau stage, growth stage, and a saturation stage, which comprised four morphological phases: adherence to the cell membrane; formation of granulated clusters spread throughout the cytoplasm; localization of granulated clusters in the perinuclear region; and formation of multivesicular body-like structures and their redistribution in the cytoplasm. Diverse quantum dots containing intracellular vesicles in the range of approximately 0.5–8 µm in diameter were observed in the cytoplasm, but none were found in the nucleus. Vesicles containing quantum dots formed multivesicular body-like structures in NIH3T3 cells after 24 hours of incubation, which were Lysotracker-negative in serum-free medium and Lysotracker-positive in complete medium. The microinjected quantum dots remained uniformly distributed in the cytosol for at least 24 hours.

**Conclusion:** Natural uptake of quantum dots in cells occurs through three accumulation stages via a mechanism requiring energy. The sharp contrast of the intracellular distribution after microinjection of quantum dots in comparison with incubation as well as the limited transfer of quantum dots from vesicles into the cytosol and vice versa support the endocytotic origin of the natural uptake of quantum dots. Quantum dots with proteins adsorbed from the culture medium had a different fate in the final stage of accumulation from that of the protein-free quantum dots, implying different internalization pathways.

**Keywords:** endocytosis, internalization, carboxyl, lysosome, protein corona, multivesicular body-like structures, ring-like vesicles, green fluorescent protein, pathway, saturation

## Introduction

An understanding of the fundamental interactions of nanoparticles with cells plays a central role in nanomedicine, as well as in terms of nanosafety issues.<sup>1</sup> Researchers have had considerable success in using nanoparticles and especially quantum dots for in vitro bioassays, labeling of fixed cells and tissue specimens, and selective imaging of membrane proteins in living cells.<sup>2</sup> On the other hand, the cytosol and various

Correspondence: Ricardas Rotomskis  
Biomedical Physics Laboratory, Institute of Oncology, Vilnius University,  
P. Baublio 3b, LT-08408, Vilnius, Lithuania  
Tel +370 5 2190908  
Fax +370 5 2720164  
Email ricardas.rotomskis@vuoi.lt

subcellular organelles house the most important biochemical processes involved in the functions of the cell. Effective delivery to the cytosol enhances the potency of anticancer drugs, stimulates the adaptive immune response, and is crucial for gene therapies involving delivery of DNA or RNA.<sup>3</sup> However, only limited progress has been made in developing quantum dot probes to perform imaging inside living cells.<sup>4</sup> A major problem is the lack of efficient methods for delivering monodispersed quantum dots into the cytoplasm of living cells.<sup>5,6</sup> The first paper on accumulation of quantum dots in cells was published more than a decade ago,<sup>7,8</sup> but the question of how quantum dots enter different cells is still open.

Methods used to date for intracellular delivery of quantum dots and a variety of other nanoparticles can be derived from three strategies,<sup>6</sup> ie: passive delivery, which relies on the inherent physicochemical properties of the quantum dot itself (coating, structure, and charge) to mediate cellular internalization; facilitated delivery, which typically involves marking the quantum dot surface with a functional molecule that can be biological in nature (such as a peptide or a protein) or with other functional chemicals, such as polymers or drugs; and direct delivery, which involves physical techniques, such as microinjection and electroporation. Intracellular uptake (passive or facilitated delivery) of quantum dots or other particles may occur via various endocytotic mechanisms,<sup>9</sup> passive permeation, and adsorptive endocytosis.<sup>10</sup> It is clear that accumulation of quantum dots in cells is a complicated issue because numerous intrinsic factors influence the uptake and intracellular transport of nanoparticles, including size, surface charge, and structure of a coating.<sup>1,11,12</sup> Analysis of results presented in the literature reveals a very wide range of values for quantum dot internalization parameters, in particular, uptake time and intracellular localization.<sup>13–24</sup> This could be due to time-dependent changes in accumulation and intracellular distribution of quantum dots taking place even in a single cell line. The interpretation of results is even more complicated in the case of *in vivo* studies where the quantum dots would be internalized by different types of cells.<sup>13</sup>

A major challenge in nanomaterial science is to develop approaches ensuring that, when administered *in vivo*, nanoparticles can be targeted to their designated site of action. However, nanoparticles in a biological environment are quickly coated by serum proteins, which affect their cellular uptake, transportation, and fate,<sup>25</sup> including the cellular response, and can have important consequences for therapeutic efficacy.<sup>26</sup> It has been reported that reduction of protein adsorption *in vivo* helps to avoid the

reticuloendothelial system.<sup>27</sup> There is still a lot to learn about cellular uptake and intracellular transport of nanoparticles in order to interpret data from *in vitro* studies unambiguously, to improve their *in vivo* use, and to facilitate the rational design of functionalized quantum dots.<sup>28</sup>

Therefore, this study was dedicated to expanding the understanding of natural quantum dot uptake by analysis of differences in accumulation between several cell lines, over wide time intervals. The focus was on intracellular localization and transportation of one type of nonfunctionalized quantum dot bearing a negatively charged coating, observing its fate after incubation in complete medium or serum-free medium, and after microinjection.

## Materials and methods

### Cell cultures

An immortalized mouse embryonic fibroblast cell line (NIH3T3, average doubling time 22 hours),<sup>29</sup> a human breast adenocarcinoma cell line (MCF-7, average doubling time 29 hours),<sup>29</sup> and a human hepatocellular carcinoma-derived cell line (HepG2, average doubling time 34 hours)<sup>29</sup> were cultured in the presence of CO<sub>2</sub> (5% v/v) at 37°C in Dulbecco's modified Eagle's medium (Gibco, Grand Island, NY) supplemented with fetal bovine serum (10% v/v), 0.1% antibiotics (stock, 1000 U/mL penicillin, 1000 µg/mL streptomycin) to obtain approximately 60% confluence. For all experiments on uptake of quantum dots, the cells were seeded in 30 mm Petri dishes at a density of 40% confluence in growth medium and allowed to grow for one day. The final 10 nM concentration of quantum dots was used in the incubation medium for all experiments.

### Quantum dots

Commercially available CdSe/ZnS quantum dots with a 5.2 nm core<sup>30</sup> eFluor™ 625 NC (Carboxyl), (Cat No 94-6364, eBioscience™ eBioscience, Inc. San Diego, CA, USA) (recommended range for excitation 350–610 nm and an emission peak at 625 nm), rendered water-dispersible with a patented poly ethylene glycol-lipid layer and carboxyl groups (total hydrodynamic radius 13–18 nm), delivered as a 10 µM aqueous solution, were used as model nanoparticles. The superficial carboxyl groups (pK<sub>a</sub> = 1.8–2.5) on the quantum dots remain deprotonated at physiological pH and form negatively charged COO<sup>−</sup> residuals.

### Confocal microscopy

Living cells were incubated in full or serum-free medium for different periods and then imaged using a confocal

microscope (Eclipse TE2000-S, C1 plus, Nikon, Tokyo, Japan) by sequential scanning with the beam of an Argon ion laser (488 nm), at  $600 \times$  total magnification using a  $60 \times$  NA 1.4 objective (Plan Apo VC, Nikon). For standard images, the three-channel RGB detector (band-pass filters 515/30 and 605/75 for green and red channel, respectively) was used. Image processing was performed using the Nikon EZ-C1 Bronze version 3.80 and ImageJ 1.41 software. Quantum dot imaging in a red spectral range (578–632 nm) was done, retaining the same parameters for all fluorescence images. All cell lines were rinsed three times with a warm Dulbecco's modified Eagle's medium before imaging.

## Steady-state fluorescence spectroscopy of intracellular uptake dynamics

The cells were incubated in Petri dishes with 10 nM of quantum dots in a serum-free medium over a time course ranging from 15 minutes to 24 hours and were kept in the incubator (37°C, 5% CO<sub>2</sub>) or on ice (4°C) to study the effect of temperature. After the appropriate time had passed, the cells were washed three times with phosphate-buffered saline (pH 7.4) and detached from their plates by trypsinization. After trypsinization, the cells were collected, centrifuged (at 500 g for 2 minutes) and resuspended in a final phosphate-buffered saline volume of 1.5 mL. The cell concentration was determined by counting the number of cells per milliliter using a hemacytometer. Quantitative analysis of quantum dot uptake into living cells was performed using a steady-state Fluorescence Lifetime spectrometer (FLS920, Edinburgh Instruments, Livingston, UK). During spectroscopic measurements, the temperature was maintained at 37°C in a temperature-controlled cuvette chamber. The cell suspension was placed in a 1 cm path length cuvette (Hellma Optics, Jena, Germany) and stirred constantly with a micro stir bar to ensure a uniform concentration of cells and to prevent sedimentation. Photoluminescence was excited at 405 nm, and excitation and emission slits were set for 5 nm. Autofluorescence of suspended cells was measured in control samples. Statistical analyses were performed using the one-way analysis of variance test, and differences were considered to be statistically significant at  $P < 0.05$ . The data used for analysis were representative results or the means of at least three independent experiments  $\pm$  the standard error of the mean.

## Microinjection

Solution for injection was prepared by diluting 0.5  $\mu$ L of quantum dots from a stock solution in 9.5  $\mu$ L of

phosphate-buffered saline. A microinjector (Eppendorf FemtoJet and CellTram Air, Hamburg, Germany) was used for direct injection of the quantum dots into the cytoplasm (injection pressure 200 hPa, rate 500  $\mu$ m/s). Confocal fluorescent images of the cells were taken immediately after injection and incubation for 24 hours (37°C, 5% CO<sub>2</sub>).

## Transfection with eGFP plasmid

Temporal transfection of NIH3T3 with enhanced green fluorescent protein (eGFP) plasmid followed the standard protocol for transfection of adherent cells. The following solutions were prepared separately: solution A, eGFP plasmid in 50  $\mu$ L of Dulbecco's modified Eagle's medium, and solution B, 1.5  $\mu$ g of Metafectene<sup>®</sup> Pro (Biontex, Martinstried, Germany) in 50  $\mu$ L of Dulbecco's modified Eagle's medium free of antibiotics. Mixed solutions were kept at room temperature for 20 minutes. The plasmid-Merafectene Pro complexes formed were added to the plates containing NIH3T3 cells. After 6 hours, the transfection mixture was removed and replaced with fresh Dulbecco's modified Eagle's medium supplemented with fetal bovine serum (10% v/v) and 0.1% antibiotics (stock, 1000 U/mL penicillin, 1000  $\mu$ g/mL streptomycin), and the plates were returned to the CO<sub>2</sub> incubator for 48 hours. Next, 3  $\mu$ L of quantum dot suspension was added to the medium on the plates, and the NIH3T3 cells were kept in the CO<sub>2</sub> incubator until analysis.

## Intracellular localization of quantum dots using LysoTracker<sup>®</sup>

NIH3T3 cells in complete and serum-free medium were treated with 10 nM quantum dots for 24 hours in a CO<sub>2</sub> incubator at 37°C, then washed three times and additionally stained for 2 hours with 50 nM of lysosome dye (LysoTracker green, Invitrogen, Carlsbad, CA). Confocal fluorescence images were recorded separately in each fluorescence channel and merged afterwards.

## Results

### Natural uptake of quantum dots

Uptake of quantum dots into NIH3T3 cells was markedly decreased at the lower temperature, indicating that the process is energy-dependent (Figure 1). The anticipated elevation of cellular uptake of carboxyl quantum dots at a temperature of 37°C also implied the active nature of the accumulation mechanism dominating over internalization of small-sized molecules via passive diffusion.<sup>31</sup>

The uptake kinetics drawn on the basis of changes in red photoluminescence intensity revealed an S-shaped (plateau,

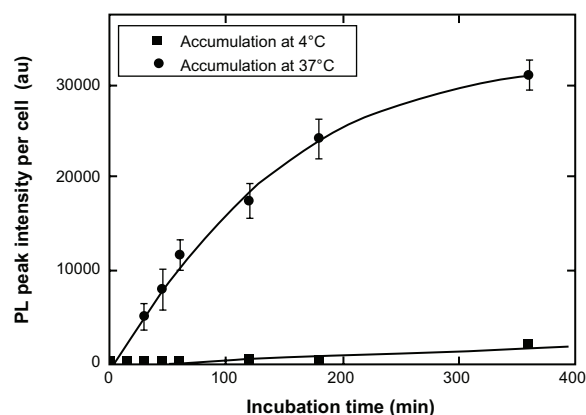


**Figure 1** Dynamics of accumulation for carboxyl-loaded quantum dots in NIH3T3 cells at 4°C and 37°C in serum-free medium.

growth, and saturation stages) dependence of accumulation of carboxyl-coated quantum dots in different cell lines (NIH3T3, HepG2, and MCF-7) on duration of incubation at 37°C (Figure 2A), but the stages were of different timing for each of the cell lines (Figure 2B). The photoluminescence

intensity of the carboxyl-coated quantum dots associated with NIH3T3 and MCF-7 cells increased with time and started to saturate after 6 hours. The photoluminescence intensity in the case of HepG2 cells remained very weak and started to increase only after 30 hours. Confocal fluorescence images taken immediately, and at 0.5, 1, 6, 24, and 48 hours after incubation of the cells with quantum dots (Figure 2C–F and Supplementary data, Figure 1) show evolution of the distribution pattern and transport vesicles of carboxyl-coated quantum dots in the cells: phase 1, adherence to the cell membrane ( $t_{inc}$  30–60 minutes, Figure 2C); phase 2, formation of granulated clusters spreading in the cytoplasm ( $t_{inc}$  0.5–6 hours, Figure 2D); phase 3, localization of granulated clusters in the perinuclear region ( $t_{inc}$  6–24 hours, Figure 2E); and phase 4, formation of multivesicular body-like structures and their redistribution in the cytoplasm ( $t_{inc}$  > 24 hours, Figure 2F). The granulated pattern of the red photoluminescence of quantum dots present inside NIH3T3 cells (assigned to phase 2, Figure 2D and Figure 3A), indicates

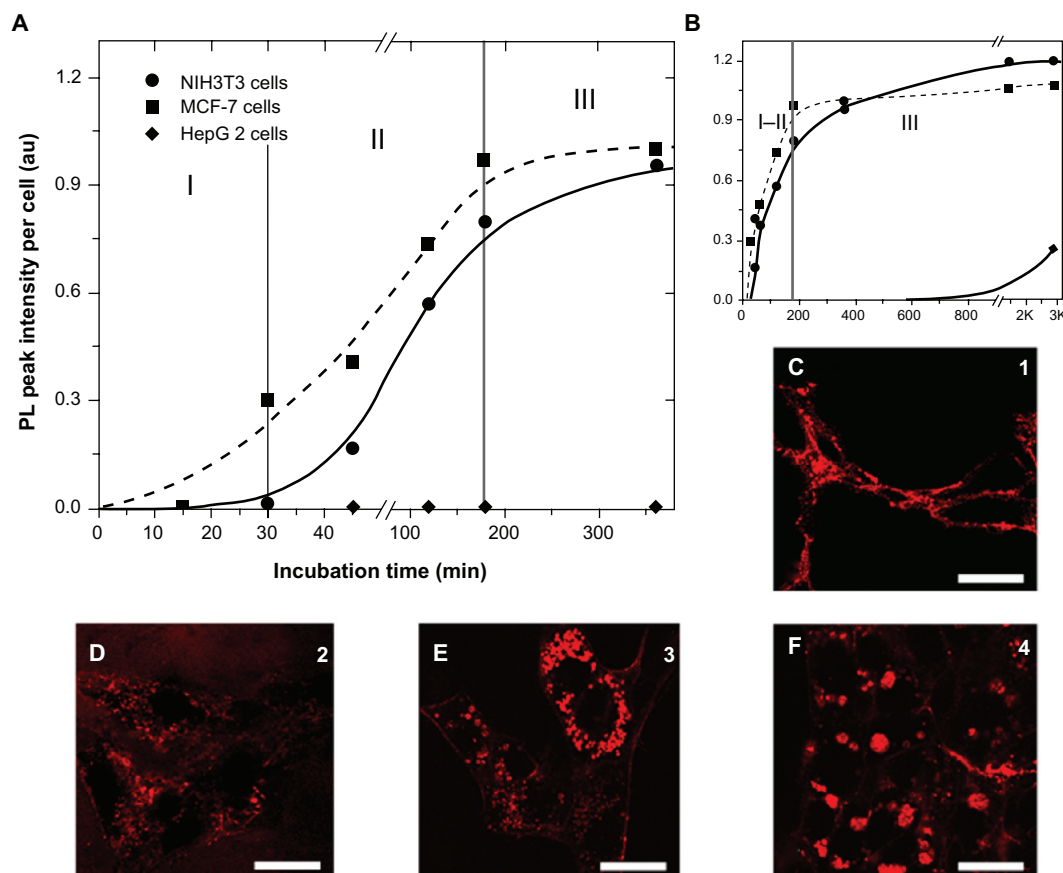


**Figure 2 (A and B)** Dynamics of internalization of carboxyl-quantum dots into NIH3T3, HepG2, and MCF-7 cells at 37°C, with indicated stages of accumulation presented in different scale range, accompanied by confocal fluorescence images of NIH3T3 cells, illustrating the observed morphological phases: (C), phase I, adherence to cell membrane; (D) phase 2, formation of vesicular structures spread in the cytoplasm; (E) phase 3, vesicle fusion and localization in the perinuclear region; (F) phase 4, formation of the multivesicular body-like structures and their redistribution in the cytoplasm.

**Note:** Serum-free medium, scale bar 20  $\mu$ m.



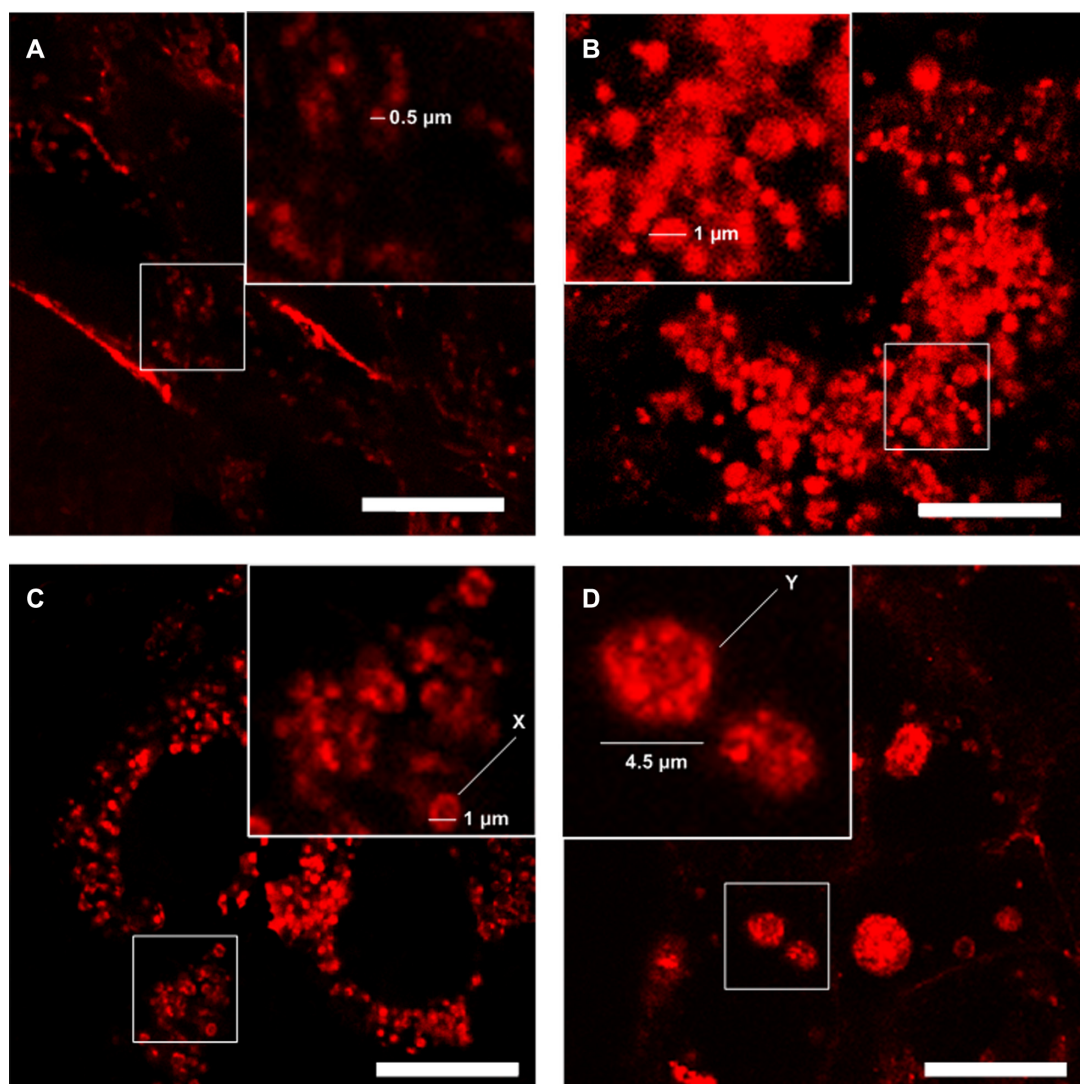


**Figure 3** Confocal fluorescence images of the types of vesicular structures formed in NIH3T3 cells during phase 2 (A), phase 3 (B and C), and phase 4 (D) of incubation with quantum dots.

**Notes:** X indicates ring-like images of vesicles with quantum dots attached to the inner surface of the vesicle without distribution throughout the volume; Y indicates large multivesicular body-like structures. Scale bar 10  $\mu\text{m}$ .

that the quantum dots were trapped in vesicular structures. The quantum dots remained inside these vesicles during the entire period of observation, and only the number of vesicles per cell increased during phases 3 and 4 (Figure 2E and F, and Figure 3B–D), as did their size and the intensity of photoluminescence.

Diverse vesicles ranging from about 0.5  $\mu\text{m}$  to 8  $\mu\text{m}$  in diameter (Figure 3) were seen on close inspection. The fluorescence images of the smallest vesicles with a diameter up to 0.5  $\mu\text{m}$  were detected during phase 2 (Figure 3A). Two different vesicle types of the same size (about 1  $\mu\text{m}$  in diameter) were observed during phase 3, ie, those fully filled with quantum dots (Figure 3B) and the ring-like vesicles with quantum dots being attached to the inner surface

without distribution throughout the cytosol (Figure 3C). The largest vesicles (approximately 5–8  $\mu\text{m}$ ) observed during phase 4 were revealed to be multivesicular body-like structures, being formed of many small vesicles completely filled with quantum dots and packed into a single large vesicle (Figure 3D).

### Direct delivery of quantum dots

The comparative study of the fate of quantum dots entering cells via passive diffusion was performed by simulating the direct delivery approach. A strikingly contrasting distribution pattern of quantum dot photoluminescence was observed in cells after intracellular microinjection (Figure 4A and B versus C). The injected quantum dots were instantly well

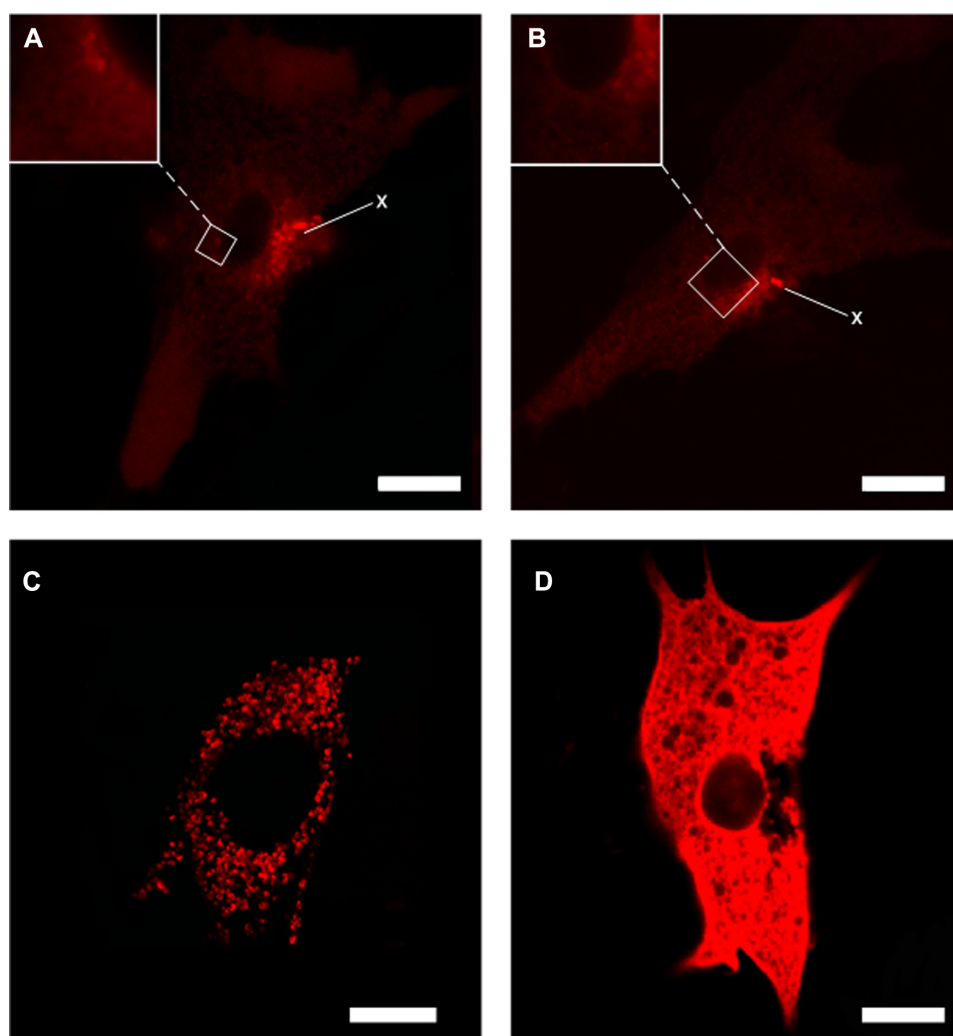


**Figure 4** Confocal fluorescence images of NIH3T3 cells taken immediately after injection of quantum dots (A), 24 hours after injection (B), and 24 hours after incubation with quantum dots (C), presented for the sake of comparison with a cell with a damaged plasma membrane (D).

**Notes:** X represents the injection site; white rectangles marks the zoomed parts shown in the inserts. Scale bar 10  $\mu$ m.

dispersed throughout the entire cytoplasm. No formation of granular structures and no visible signs of aggregation were seen (Figure 4A). Formation of quantum dot-containing vesicular structures was not observed afterwards either (Figure 4B). In fact, such distribution of injected quantum dots was found to be similar to the intracellular distribution pattern of quantum dot photoluminescence observed in a cell with a damaged plasma membrane during incubation with quantum dots (Figure 4D).

### Fate of intracellular quantum dots

The observed time-dependent restructuring of quantum dot-containing vesicles during natural uptake and accumulation (changes in size of vesicles and formation of multivesicular body-like structures) prompted us to investigate the intracellular migration of quantum dots, possible fusion of

quantum dot-containing vesicles, and likelihood of quantum dots becoming entrapped inside vesicles escaping into the cytosol. eGFP-transfected cells have been used to clarify those processes. Transfection in itself had no influence on the phases of quantum dot accumulation in cells or on formation and reshaping of red-luminescing endosomes (Figure 5B). Dark and red-luminescing endosomes were detected on the background of the green fluorescence in eGFP transfected cells after 24 hours of keeping them in a growth medium with quantum dots (Figure 5A). Close inspection of the vesicles formed revealed small (about 0.5  $\mu$ m) vesicles inside larger (about 1.5  $\mu$ m) dark endosomes (Figure 5C), implying possible fusion of endosomes containing quantum dots with endosomes without quantum dots. However, no trace of red photoluminescence of quantum dots dispersed across the entire cytosol was detected (Figure 5B and C), as in the case

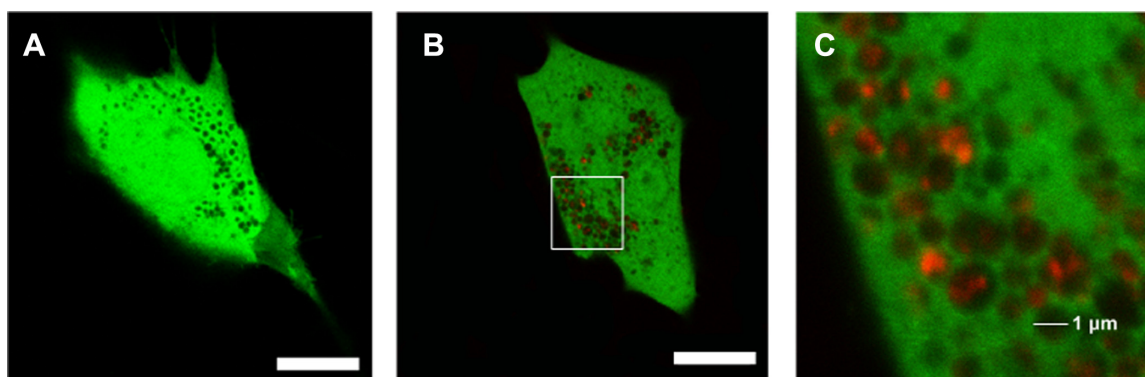


**Figure 5** Confocal fluorescence images of enhanced green fluorescent protein-transfected NIH3T3 cells (A) and NIH3T3 cells at 24 hours after incubation with quantum dots (B). (C) is a zoomed part of (B), shown with white rectangle. **Note:** Scale bar 10  $\mu$ m.

of microinjection of quantum dots (Figure 4A and B), and no appearance of a yellow color caused by colocalization of red quantum dots with green eGFP was found. The presence or absence of protein in the growth medium was found to have no influence on these observations.

Additional investigation of the role of incubation conditions in the fate of quantum dots inside NIH3T3 cells was performed using a fluorescent cell-permeant acidic organelle-selective marker, ie, Lysotracker green. The Lysotracker probes, which comprise a fluorophore linked with a weak base that is only partially protonated at neutral pH, freely penetrate cell membranes and are typically used to mark organelles (lysosomes) at acidic pH. Because the same four morphological phases were observed when incubating the cells with quantum dots in complete or serum-free medium, Lysotracker was used to identify the ability of quantum dots to reach the lysosomal compartments.

Confocal microscopy of NIH3T3 cells after 24 hours of incubation showed that that fluorescence images of quantum dot-containing vesicles and Lysotracker green-stained organelles were matched in complete medium (Figure 6A–C), but quantum dots and Lysotracker were not colocalized in fluorescent images taken in serum-free medium. Quantum dots were observed in Lysotracker-negative vesicles with, most likely, higher internal pH (Figure 6E–G). The Lysotracker-positive compartments without quantum dots were still observed throughout the cytoplasm of the cells (Figure 6E).

It was also of interest to determine whether cells have removal pathways for quantum dots once they have been taken up or whether accumulation of quantum dots in the lysosomes could lead to their degradation. However, extracellular release of the vesicle contents was never observed in any tested cell line (for NIH3T3 cells, see Supplementary data, Figure 2). It is of note that all the treated cells

remained viable for at least 96 hours (for NIH3T3 cells see Supplementary data, Figure 3) without any signs of quantum dot-induced toxicity. Further, no traces of quantum dots were found in the nucleus (Supplementary video available at <http://youtu.be/-Vma-7sGw0Y>).

## Discussion

The effect of temperature on the accumulation dynamics of nontargeted quantum dots indicates that quantum dots are internalized by an energy-requiring membrane transport process, presumably an energy-requiring endocytotic mechanism which is not effective at 4°C.<sup>32,33</sup> Cell membrane lipids have a tendency to form a “gel-like” phase, which inhibits both natural uptake and passive diffusion of nanoparticles into the cell.<sup>34</sup> It is known that diffusion through the lipid bilayer is characterized as an instantaneous linear<sup>35</sup> and nonsaturable process.<sup>31</sup> However, with increasing temperature, the plateau and saturation stages observed in the process of accumulation of nontargeted quantum dots indicates that passive diffusion through the intact cell plasma membrane is negligible, even if the size of biologically inert quantum dots implies that they could enter the cell via pore defects.<sup>36</sup>

Despite time-related differences, the distribution of nontargeted quantum dots followed similar accumulation stages and morphological phases in the different cell lines (NIH3T3, HepG2 and MCF-7). It is worth mentioning that the morphological phases of accumulation of quantum dots were not equally clearly expressed in the cell lines studied. The main reasons could be the different physiology of the cell lines and cell type-specific surface receptors<sup>37</sup> (Figure 2B, Supplementary data, Figure 1E–H). The observed variations in timing of uptake between the cell lines (Figure 2A and B) may also be influenced by cell-related specificity of internalization mechanisms for quantum dots.

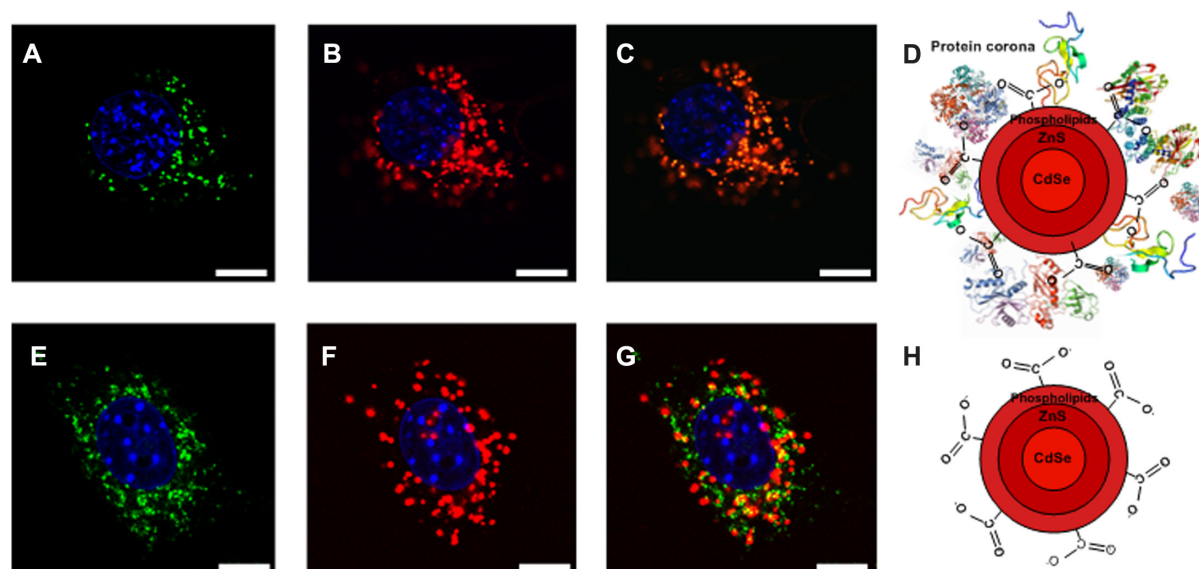


**Figure 6** Confocal fluorescence images of quantum dot localization in NIH3T3 cells after 24 hours of incubation in complete medium (A) registered in green channel showing green fluorescence of Lysotracker, (B) in red, showing red fluorescence of quantum dots (C), combined and incubated in serum-free medium [(E) registered in green channel, (G) in red, and (F) combined]. Nuclei stained with DAPI, scale bar 10  $\mu$ m. (D) and (H) are schematic presentations of quantum dots with and without adsorbed proteins, respectively.

It should be noted that phases 1 and 2 of quantum dot distribution in the cells were found earlier in the studies reported by Hoshino et al,<sup>16</sup> Clift et al,<sup>20</sup> and Jiang et al,<sup>19</sup> Kelf et al,<sup>14</sup> Williams et al,<sup>15</sup> and Corsi et al,<sup>17</sup> which showed formation of vesicular structures spread in the cytoplasm corresponding to phase 2. Phase 3, ie, localization of vesicular structures in the perinuclear region, was described by Zhang et al<sup>22</sup> and Xiao et al,<sup>23</sup> and reviewed by Parak et al.<sup>33</sup> Phase 4 resembles the data on formation of multivesicular body-like structures and their redistribution in cytoplasm presented by Yuan et al<sup>18</sup> and Jiang et al.<sup>19</sup> However, there has been no presentation of an overall picture illustrating the time-dependent nature of natural uptake and distribution of nontargeted negatively charged quantum dots in living cells.

On the basis of the results presented here, we suggest a scheme for a potential natural mechanism of intracellular uptake of nontargeted quantum dots as illustrated in Figure 7 and comprised of the four major phases described above. Internalization of quantum dots can occur via several possible primary steps, ie, adsorption of proteins from the culture medium onto the surface of the quantum dots, followed by their internalization via receptor-mediated pathways<sup>14</sup> or nonspecific binding and clustering of the nanoparticles near cationic sites on the plasma membrane, triggering receptors and inducing subsequent endocytosis<sup>12</sup> (Figure 7). The uptake process begins with adherence of quantum dots to cell surface receptors present in the plasma membrane. Following energy-dependent internalization during phase 1, this

complex then enters the cells in the form of cargo located inside receptor-coated structures called endocytotic vesicles. Adherence of quantum dots onto the membrane being observed only during phase 1 (Figure 2C–F) together with a certain specificity in quantum dot uptake (Figure 5C), as well as its saturation in time (Figure 2B), which cannot be explained by doubling time or cell division given that the saturation stage was observed not later than 6 hours after incubation and sufficient amounts of quantum dots were present in the medium, indicate a gradual interruption of the receptor sorting and recycling steps. To sustain internalization, the receptors must be recycled back to the external membrane, which takes time and lengthens the internalization rate. Consequently, the reduced number of available receptors that a nanoparticle triggers when it adheres to the membrane can also play a suppressive role during the process of internalization followed by translocation of a loaded vesicle inside the cell.<sup>38</sup> Variations in the amount of plasma membrane receptors between the different cell lines could contribute to the time-related differences observed in the uptake phases of quantum dots.

Independently of the mode of entry at phase 2, endocytosed cargo is usually delivered to early endosomes.<sup>39</sup> This process is followed by their controlled migration (against a concentration gradient), fusion, and localization in the perinuclear region (phase 3), close to the Golgi complex and microtubule organizing center.<sup>40,41</sup> Afterwards, these early endosomes mature into late endosomes (phase 4), which spread into the cytoplasm and



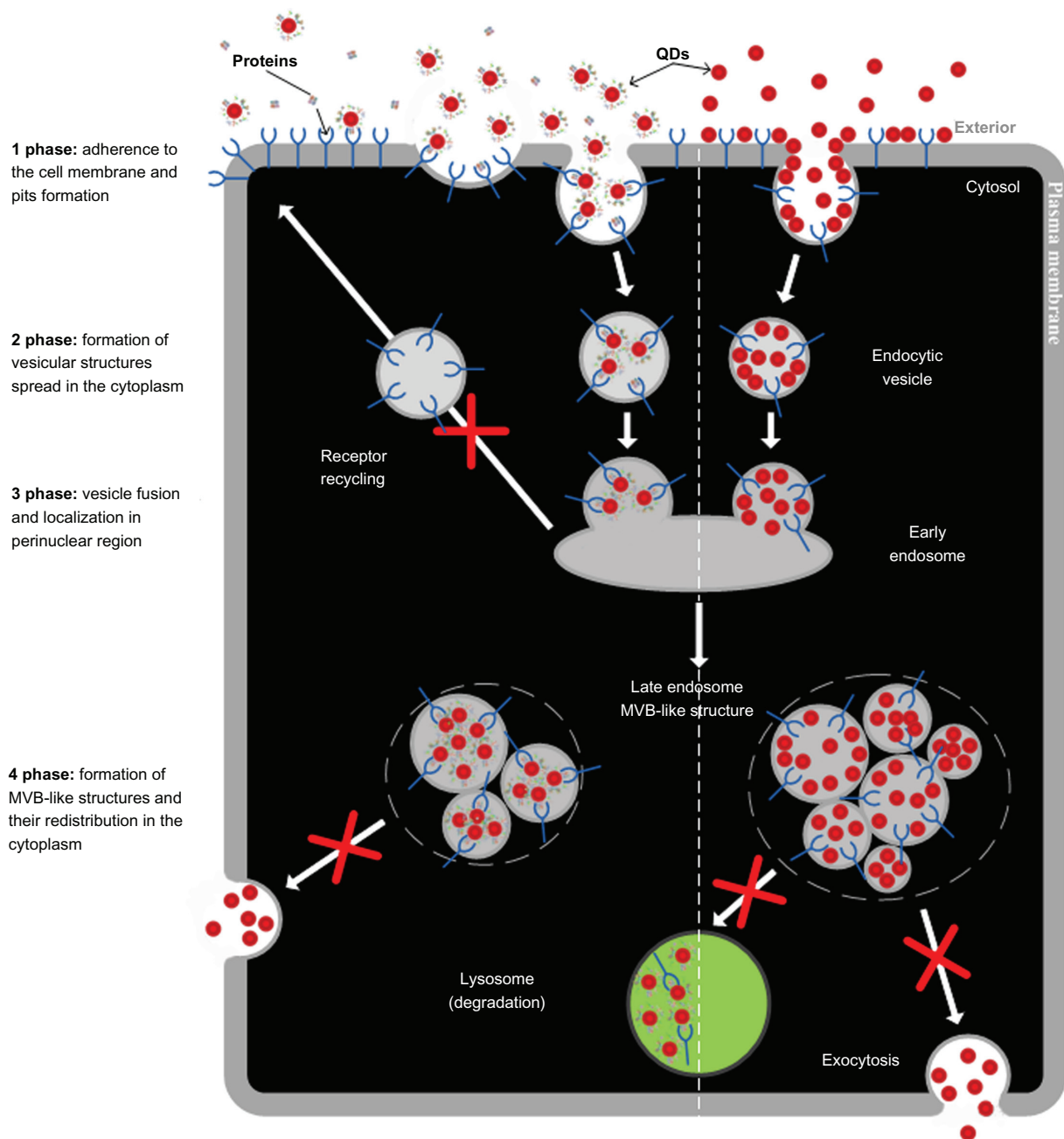


**Figure 7** Schematic representation of intracellular fate of nontargeted carboxyl-coated quantum dots: uptake, transportation, and intracellular localization.

**Notes:** Blue “Y” marks the receptor; the steps which were not observed during experiments but commonly take place are marked in red as “X”.

form long-lived multivesicular body-like structures distributed uniformly throughout the cytoplasm (Supplementary data, Figure 3). According to the observed sizes and types of quantum dot-containing vesicles, they can be categorized into three types: endocytotic vesicles, (up to 1  $\mu\text{m}$  in diameter, formation time 15–60 minutes),<sup>42</sup> which merge into larger vesicles by homotypic fusion; early endosomes (up to 5  $\mu\text{m}$  in diameter, formation time more than one hour), which are mainly spherical;<sup>43</sup> and late endosomes/multivesicular body-like structures with the presence of intraluminal vesicles.<sup>44</sup>

Direct delivery of quantum dots into cells is very limited in its throughput and is not suited to manipulation of tens to hundreds of cells at a time, but is valuable for gaining new research insights. This alternative technique allows delivery of very small sample volumes (usually femtoliters) directly into the cytoplasm of individual cells, avoiding reaction with the plasma membrane, which is the main barrier and cause of intracellular vesicle formation during natural uptake. In contrast with natural uptake, microinjected quantum dots underwent no changes and remained uniformly distributed in

the cytosol during the observation period (at least 24 hours). Moreover, experiments with eGFP transfected cells confirmed the suggestion that quantum dots entrapped inside vesicles during endocytosis could not escape to the cytosol. Vesicle fusion evident in phase 4 (Figure 2C) and in the experiments on eGFP transfected cells (Figure 5C), together with the effect of temperature on intracellular quantum dot accumulation, clearly demonstrate that natural uptake of quantum dots is impossible without endocytosis. Moreover, transfer of quantum dots from endocytotic vesicles into the cytosol and vice versa is limited.

The three accumulation stages and four phases of intracellular distribution of quantum dots were identified by confocal microscopy independently of the content of the medium, but Lysotracker experiments revealed differences in the fate of the quantum dots. Examination of the intracellular trafficking of quantum dots entrapped inside the vesicles revealed that the fate of quantum dots was highly dependent on the content of the incubation medium, affecting the primary steps of uptake, ie, quantum dots incubated with cells in serum-free medium did not fuse with lysosomes (Figure 6E–G), while quantum dots incubated with cells in complete medium were fully colocalized with lysosomes (Figure 6A–C). Partial colocalization was reported in serum-free medium by Barua et al,<sup>13</sup> with a significant fraction of quantum dots being localized in Lysotracker-negative vesicles, but the nature of these compartments was not identified. Furthermore, it has been presumed that the acidic nature of the cargo present in these vesicles, ie, carboxylated quantum dots, could contribute to acidification of these vesicles, which in turn targets them for strong staining with the reagent. Some cellular localization studies performed using nonacidic nanoparticles<sup>45,46</sup> showed that these nanoparticles did not colocalize with either early endosomes or lysosomes. Therefore, the effect of the quantum dot coating on intravesicular pH must be taken into account for interpretation of the results of intracellular localization.

The observed saturation of accumulation during incubation in full medium most likely occurred due to the protective effect of adherent proteins on the surface of the quantum dots (Figure 6D), providing them with sufficient stabilization.<sup>47</sup> Otherwise, upon entry into lysosomes, quantum dots would have been degraded, causing inactivation of cells (contrary to the observed viability of cells even after 96 hours of incubation with quantum dots, Supplementary data, Figure 3), because quantum dots are not stable in an acidic environment<sup>48,49</sup> and the core/shell elements are highly toxic to cells. The fate of highly stable, long-lived endocytotic

structures is the focus of current discussion<sup>50,51</sup> and needs further investigation.

Differences in colocalization with a lysosome marker observed between nontargeted (protein-free) quantum dots (Figure 6H) and quantum dots possessing a protein corona<sup>1</sup> (Figure 6D) imply that these quantum dots are, most likely, recognized differently by the cells and internalized by different pathways (Figure 7). Also, it should be noted that uptake of quantum dots does not depend only on their intrinsic properties, such as core material, shape, size, or charge, which are mostly reviewed in ongoing studies. The uptake, internalization pathway, and fate of the same quantum dots are also dependent on external factors (eg, content of the incubation medium), highlighting the variability of localization of the same material at the whole body, organ system, tissue, cell, and organelle levels, depending on the identity, organization, and residence time of the protein corona at the nanoparticle surface and emphasizing the need to develop “cloaked” nanoparticles as long-circulating carriers for improved applicability *in vivo*.

## Conclusion

Nontargeted negatively charged quantum dots were internalized by NIH3T3 cells via an energy-requiring endocytotic mechanism. The natural mechanism of intracellular uptake of nontargeted quantum dots is comprised of three major stages, ie, a plateau stage, growth stage, and saturation stage, accompanied with four morphological phases: adherence to the cell membrane; formation of granulated clusters spread throughout the cytoplasm; localization of granulated clusters in a perinuclear region; and formation of multivesicular body-like structures and their redistribution in the cytoplasm (Figures 2 and 7). The three stages were observed in all cell lines studied, but varied in the timing and amount of quantum dots accumulated for each cell line (Figure 2, Supplementary data, Figure 1).

Unlike with natural uptake, the injected quantum dots were diffusely spread inside the cells throughout the cytosol without any specificity (Figure 4). In addition, observations of intracellular trafficking of the quantum dots after the microinjection procedure together with the experiments on eGFP-transfected cells clearly demonstrate that the quantum dots can neither enter into vesicles from the cytosol nor escape into the cytosol, being entrapped inside the vesicles during endocytosis (Figure 5).

The natural uptake of nontargeted quantum dots bearing a negative coating thus revealed some characteristic features, ie, not only its commonly accepted dependence on the

intrinsic properties of nanoparticles, but also the properties of the external medium, low rate of accumulation, breakage of the quantum dot transportation route at phase 3, formation of ring-like shaped luminescence of vesicles with quantum dots present on membranes, and formation of long-lived multivesicular body-like structures.

All these findings provide an overall framework for future studies to clarify fully the kinetic processes involved in uptake of quantum dots by different cell types. Fundamental questions, such as the role of the protein corona in directing uptake and the internal structure of quantum dots containing vesicles regulating their intracellular localization, need further investigation for future development of in vivo applications, because endocytosis is the primary route of cellular uptake for small drugs and macromolecular therapeutics. At this present time, we believe that nontargeted quantum dots can be used for nonspecific imaging of cells but not for drug transfer because they are trapped into vesicles during uptake. For medical use, it would be necessary to tailor nanoparticles in a way that would prevent entrapment in the vesicles or to use artificial injection methods (such as electroporation, sonoporation, or photochemical internalization), enabling them to enter the cytoplasm, avoiding the first mechanical barrier, ie, the plasma membrane, and reach intracellular targets.

## Acknowledgments

This research was supported by the Norwegian Financial Mechanism and Republic of Lithuania within the Multifunctional Nanoparticles for Specific Noninvasive Early Diagnostics and Treatment of Cancer project (contract LT0036) and by the Postdoctoral Fellowship Implementation in Lithuania project (VP1-3.1-ŠMM-01-V-01-001).

## Disclosure

The authors report no conflicts of interest in this work.

## References

- Lundqvist M, Stigler J, Elia G, Lynch I, Cedervall T, Dawson KA. Nanoparticle size and surface properties determine the protein corona with possible implications for biological impacts. *Proc Natl Acad Sci U S A*. 2008;105:14265–14270.
- Smith AM, Duan H, Mohs AM, Nie S. Bioconjugated quantum dots for in vivo molecular and cellular imaging. *Adv Drug Deliv Rev*. 2008;60:1226–1240.
- Massignani M, LoPresti C, Blanz A, et al. Controlling cellular uptake by surface chemistry, size, and surface topology at the nanoscale. *Small*. 2009;5:2424–2432.
- Massignani M, Canton I, Sun T, et al. Enhanced fluorescence imaging of live cells by effective cytosolic delivery of probes. *PLoS One*. 2010;5:e10459.
- Jin S, Hu Y, Gu Z, Liu L, Wu H. Application of quantum dots in biological imaging. *J Nanomater*. 2011;2011:834139.
- Delehanty JB, Mattoussi H, Medintz IL. Delivering quantum dots into cells: strategies, progress and remaining issues. *Anal Bioanal Chem*. 2009;393:1091–1105.
- Chan WC, Nie S. Quantum dot bioconjugates for ultrasensitive nonisotopic detection. *Science*. 1998;281:2016–2018.
- Bruchez M Jr, Moronne M, Gin P, Weiss S, Alivisatos AP. Semiconductor nanocrystals as fluorescent biological labels. *Science*. 1998;281:2013–2016.
- Zaki NM, Tirelli N. Gateways for the intracellular access of nanocarriers: a review of receptor-mediated endocytosis mechanisms and of strategies in receptor targeting. *Expert Opin Drug Deliv*. 2010;7:895–913.
- Qaddoumi MG, Ueda H, Yang J, Davda J, Labhasetwar V, Lee VH. The characteristics and mechanisms of uptake of PLGA nanoparticles in rabbit conjunctival epithelial cell layers. *Pharm Res*. 2004;21:641–648.
- Zhao F, Zhao Y, Liu Y, Chang X, Chen C, Zhao Y. Cellular uptake, intracellular trafficking, and cytotoxicity of nanomaterials. *Small*. 2011;7:1322–1337.
- Verma A, Stellacci F. Effect of surface properties on nanoparticle-cell interactions. *Small*. 2010;6:12–21.
- Barua S, Rege K. Cancer-cell-phenotype-dependent differential intracellular trafficking of unconjugated quantum dots. *Small*. 2009;5:370–376.
- Kelf TA, Sreenivasan VK, Sun J, Kim EJ, Goldys EM, Zvyagin AV. Non-specific cellular uptake of surface-functionalized quantum dots. *Nanotechnology*. 2010;21:285105.
- Williams Y, Sukhanova A, Nowostawska M, et al. Probing cell-type-specific intracellular nanoscale barriers using size-tuned quantum dots. *Small*. 2009;5:2581–2588.
- Hoshino A, Hanaki K, Suzuki K, Yamamoto K. Applications of T-lymphoma labeled with fluorescent quantum dots to cell tracing markers in mouse body. *Biochem Biophys Res Commun*. 2004;314:46–53.
- Corsi F, De Palma C, Colombo M, et al. Towards ideal magnetofluorescent nanoparticles for bimodal detection of breast-cancer cells. *Small*. 2009;5:2555–2564.
- Yuan Y, Liu C, Qian J, Wang J, Zhang Y. Size-mediated cytotoxicity and apoptosis of hydroxyapatite nanoparticles in human hepatoma HepG2 cells. *Biomaterials*. 2010;31:730–740.
- Jiang W, Kim BY, Rutka JT, Chan WC. Nanoparticle-mediated cellular response is size-dependent. *Nat Nanotechnol*. 2008;3:145–150.
- Clift MJ, Brandenberger C, Rothen-Rutishauser B, Brown DM, Stone V. The uptake and intracellular fate of a series of different surface coated quantum dots in vitro. *Toxicology*. 2011;286:58–68.
- Jiang X, Röcker C, Hafner M, Brandholt S, Dörlich RM, Nienhaus GU. Endo- and exocytosis of zwitterionic quantum dot nanoparticles by live HeLa cells. *ACS Nano*. 2010;4:6787–6797.
- Zhang LW, Monteiro-Riviere NA. Mechanisms of quantum dot nanoparticle cellular uptake. *Toxicol Sci*. 2009;110:138–155.
- Xiao Y, Forry SP, Gao X, Holbrook RD, Telford WG, Tona A. Dynamics and mechanisms of quantum dot nanoparticle cellular uptake. *J Nanobiotechnology*. 2010;8:13.
- Im J, Maiti KK, Kim W, Kim KT, Chung SK. Cellular uptake properties of the complex derived from quantum dots and G8 molecular transporter. *Bull Korean Chem Soc*. 2011;32:1282–1292.
- Prapainop K, Witter DP, Wentworth P. Chemical approach for cell-specific targeting of nanomaterials: small-molecule-initiated misfolding of nanoparticle corona proteins. *J Am Chem Soc*. 2012;134:4100–4103.
- Dobrovolskaia MA, Patri AK, Zheng J, et al. Interaction of colloidal gold nanoparticles with human blood: effects on particle size and analysis of plasma protein binding profiles. *Nanomedicine*. 2009;5:106–117.
- Guo S, Huang L. Nanoparticles escaping RES and endosome: challenges for siRNA delivery for cancer therapy. *J Nanomater*. 2011;2011:742895.
- Ho YP, Leong KW. Quantum dot-based theranostics. *Nanoscale*. 2010;2(1):60–68.
- ATCC-LGC Standards Partnership. NIH/3T3 (CRL-1658); Hep G2 (HB-8065) and MCF-7 (HTB-22). Available from: <http://www.lgcstandards-atcc.org/>. Accessed May 7, 2012.

30. Yu W, Qu L, Guo W, Peng X. Experimental determination of the size dependent extinction coefficients of high quality CdTe, CdSe and CdS nanocrystals. *Chem Mater*. 2003;15:2854–2860.
31. Sugano K, Kansy M, Artursson P, et al. Coexistence of passive and carrier-mediated processes in drug transport. *Nat Rev Drug Discov*. 2010;9:597–614.
32. Silverstein SC, Steinman RM, Cohn ZA. Endocytosis. *Annu Rev Biochem*. 1977;46:669–722.
33. Parak WJ, Pellegrino T, Plank C. Labelling of cells with quantum dots. *Nanotechnology*. 2005;16:9–25.
34. Shapero K, Fenaroli F, Lynch I, Cottell DC, Salvati A, Dawson KA. Time and space resolved uptake study of silica nanoparticles by human cells. *Mol Biosyst*. 2011;7:371–378.
35. Eze M, McElhaney RN. The effect of alterations in the fluidity and phase state of the membrane lipids on the passive permeation and facilitated diffusion of glycerol in *Escherichia coli*. *J Gen Microbiol*. 1981;124:299–307.
36. Dobson PD, Kell DB. Carrier-mediated cellular uptake of pharmaceutical drugs: an exception or the rule? *Nat Rev Drug Discov*. 2008;7:205–220.
37. Douglas KL, Piccirillo CA, Tabrizian M. Cell line-dependent internalization pathways and intracellular trafficking determine transfection efficiency of nanoparticle vectors. *Eur J Pharm Biopharm*. 2008;68:676–687.
38. Rejman J, Oberle V, Zuhorn IS, Hoekstra D. Size-dependent internalization of particles via the pathways of clathrin and caveolae-mediated endocytosis. *Biochem J*. 2004;377(Pt 1):159–169.
39. Grant BD, Donaldson JG. Pathways and mechanisms of endocytic recycling. *Nat Rev Mol Cell Biol*. 2009;10:597–608.
40. Damalakiene L, Bagdonas S, Rotomskis R, Karabanovas V, Ger M, Valius M. Influence of growth factor on internalization pathway of quantum dots into cells: PDGF effects internalization of QDs. Presented at the 9th Annual Institute of Electrical and Electronics Engineers Conference, July 26–30, 2009, Genoa, Italy.
41. Dikic I. *Endosomes Molecular Biology Intelligence Unit*. New York, NY: Landes Bioscience; 2006.
42. Pavelka M, Roth J. *Functional Ultrastructure: An Atlas of Tissue Biology and Pathology*, 2nd ed. New York, NY: Springer Wien; 2010.
43. Abe K, Takano H, Ito T. Appearance of peculiar multivesicular bodies in the principal cells of the epididymal duct after efferent duct cutting in the mouse. *Arch Histol Jpn*. 1984;47:121–135.
44. Sorkin A, von Zastrow M. Endocytosis and signalling: intertwining molecular networks. *Nat Rev Mol Cell Biol*. 2009;10:609–622.
45. Johnston HJ, Semmler-Behnke M, Brown DM, Kreyling W, Tran L, Stone V. Evaluating the uptake and intracellular fate of polystyrene nanoparticles by primary and hepatocyte cell lines in vitro. *Toxicol Appl Pharmacol*. 2010;242:66–78.
46. Ray A, Koo Lee YE, Epstein T, Kim G, Kopelman R. Two-photon nano-PEBBLE sensors: subcellular pH measurements. *Analyst*. 2011;136:3616–3622.
47. Poderys V, Matulionyte M, Selskis A, Rotomskis R. Interaction of water-soluble CdTe quantum dots with bovine serum albumin. *Nanoscale Res Lett*. 2011;6:9.
48. Karabanovas V, Zakarevicius E, Sukackaite A, Streckyte G, Rotomskis R. Examination of the stability of hydrophobic (CdSe)ZnS quantum dots in the digestive tract of rats. *Photochem Photobiol Sci*. 2008;7:725–729.
49. Kulvietis V, Streckyte G, Rotomskis R. Spectroscopic investigations of the quantum dot stability in different aqueous media. *Lithuanian Journal of Physics*. 2011;51:163–171.
50. Iversena T, Skotland T, Sandvig K. Endocytosis and intracellular transport of nanoparticles: Present knowledge and need for future studies. *Nano Today*. 2011;6:176–185.
51. Hayer A, Stoeber M, Ritz D, Engel S, Meyer HH, Helenius A. Caveolin-1 is ubiquitinated and targeted to intraluminal vesicles in endolysosomes for degradation. *J Cell Biol*. 2010;191:615–629.



## Supplementary data

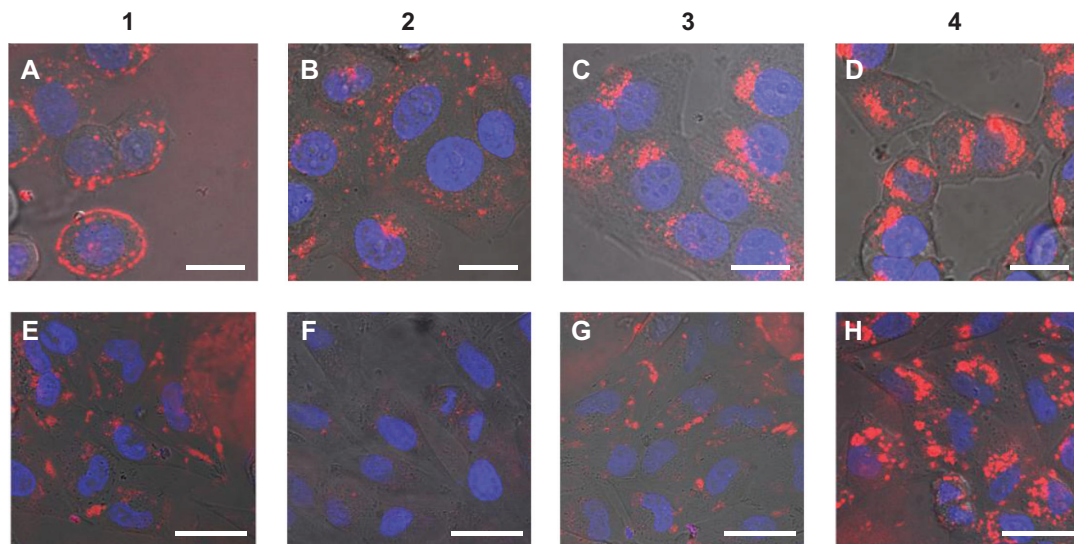


**Figure S1** Confocal fluorescence images overlaid with phase contrast images of quantum dots accumulation dynamics in MCF-7 (A-D) and HepG2 (E-H) cells. Nuclei stained with DAPI, scale bar 20 μm.

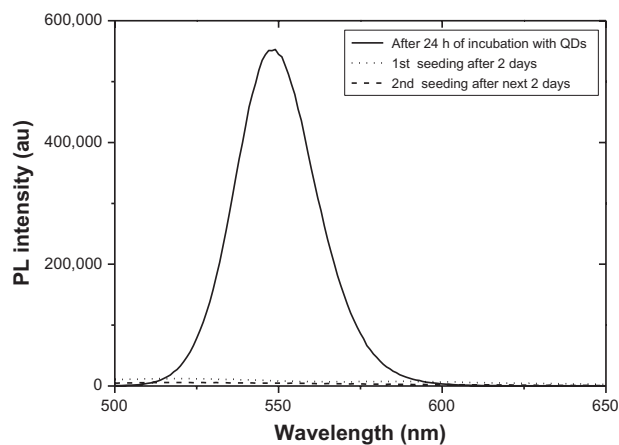


**Figure S2** Photoluminescence spectra of complete growth medium used for incubation of NIH3T3 cells with QDs and the medium used after reseeding the NIH3T3 with internalized quantum dots. Excitation wavelength 405 nm.

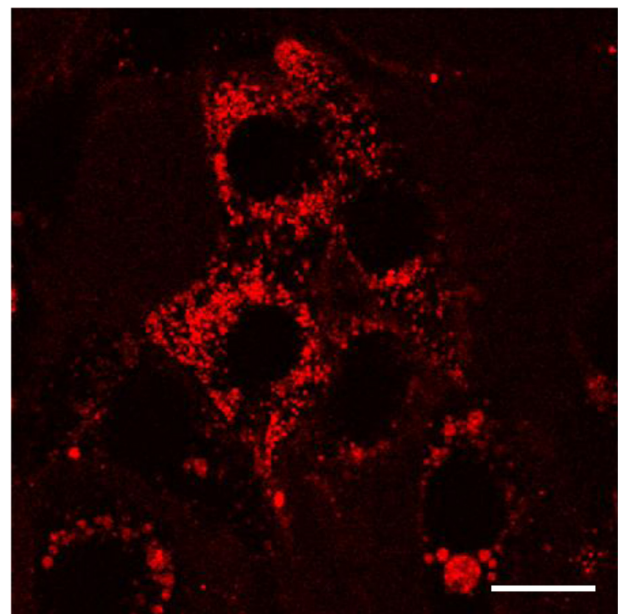


**Figure S3** Confocal fluorescence image of NIH3T3 cells after 96 hours incubation with quantum dots in full medium. Scale bar 10 μm.

**International Journal of Nanomedicine****Dovepress****Publish your work in this journal**

The International Journal of Nanomedicine is an international, peer-reviewed journal focusing on the application of nanotechnology in diagnostics, therapeutics, and drug delivery systems throughout the biomedical field. This journal is indexed on PubMed Central, MedLine, CAS, SciSearch®, Current Contents®/Clinical Medicine,

Journal Citation Reports/Science Edition, EMBase, Scopus and the Elsevier Bibliographic databases. The manuscript management system is completely online and includes a very quick and fair peer-review system, which is all easy to use. Visit <http://www.dovepress.com/testimonials.php> to read real quotes from published authors.

Submit your manuscript here: <http://www.dovepress.com/international-journal-of-nanomedicine-journal>